

Supporting Information for

The Bimetallic Effect Promotes the Activity of Rh in Catalyzed Selective Hydrogenation of Phenol

*Shiwei Li^{a,b}, Huachao Zhao^{a,b}, Wei Ran^a, Jingfu Liu^{a,b,c} and Rui Liu^{*a,b,c}*

^a State Key Laboratory of Environmental Chemistry and Ecotoxicology, Research Center for Eco-Environmental Sciences, Chinese Academy of Sciences, Beijing 100085, China

^b School of Environment, Hangzhou Institute of Advanced Study, UCAS, Hangzhou 310024, China

^c College of Resources and Environment, University of Chinese Academy of Sciences, Beijing 100049, China

Table of Content

Methods	S2
Additional Discussion.....	S6
Supporting Figure S1-S19	S8
Supporting Table S1-S3	S18
Reference	S21

Methods

Materials. HAuCl₄, HNO₃, HCl and KBH₄ were purchased from Sinopharm Chemical Reagent Co. (Beijing, China). Phenol, Cyclohexanone and Cyclohexanol was purchased from Alfa Aesar. Na₂PdCl₄, RhCl₃·3H₂O, 2,6-dimethylphenylisocyanide(2,6-DMPI), Rh/Al₂O₃, AgNO₃ and Triton X-114 (TX-114) were purchased from Sigma-Aldrich. All chemicals were used as received without further purification. Water with a resistivity of 18.2 MΩ·cm was used for all experiments.

Synthesis of Au@Rh, Au@RhPd, Au@Ag@RhPd Monolayer Catalysts. The ultrathin Au NWs were synthesized according to our reported procedure.¹ For the preparation of Au@M core-shell NWs, 3 mL of 1 mM ice-cold precursor solution (Na₂CiO₄, RhCl₃·3H₂O or Pd/Rh mixture) was added into 10.0 mL dispersion of freshly synthesized Au NWs dropwise while stirring. In the case of Au@Ag@M, 3.0 mL of 1 mM ice-cold AgNO₃ solution was added into a 10.0 mL dispersion of freshly synthesized Au NWs while stirring, followed by the addition of 3 mL of 1 mM ice-cold Na₂CiO₄, RhCl₃·3H₂O or Pd/Rh mixture solution.

In each of these cases, the coverage is monolayer and varying the ratio of palladium and rhodium to obtain different catalysts.

Synthesis of Rh Nanoparticles

The synthesis of Rh nanoparticles was similar to that of Au NWs. Briefly, 45 mL mixture solution containing 0.05 mmol $\text{RhCl}_3 \cdot 3\text{H}_2\text{O}$ and 0.025 mg TX-114 was stirred 30 minutes in an ice bath. Then 5 mL of 100 mM KBH_4 solution was added quickly with vigorous stirred.

CO-Stripping Experiment

50 μL of the catalyst was dripped on the glassy carbon electrodes, after air-dried, 3 μL of 10% Nafion solutions were added to form Nafion films. The prepared electrodes were activated by cyclic voltammetry between -0.25 to 1.0 V (vs Ag/AgCl) in N_2 -saturated 0.1M HClO_4 solutions. The platinum wire electrodes and the Ag/AgCl electrodes were used as the counter electrodes and the working electrodes, respectively. After being chemically adsorbed on the metal surface atoms, CO was peeled off at a scanning speed of $50 \text{ mV} \cdot \text{s}^{-1}$. The CO-stripping experiment was performed to verify the existence of Rh atoms on the Pd NWs.

Electrochemical experiment

With the stepwise deposition of Pd on Au NWs, the relative area of the AuO_x reduction peak further decreased, and a new reduction peak associated the reduction of PdO_x emerged at lower potential. When the amount of Pd reached 1.0 ML, the AuO_x reduction peak was completely disappeared (Figure S3).

Characterization of Catalysts and SERS Experiment of chemisorbed 2,6-DMPI on NWs

TEM (JEM-2100F) and Cs-STEM were used to characterize the morphology of as-prepared NWs. EDS-Mapping were performed to characterize the surface structure.

In the SERS experiment, 100 μL 2,6-DMPI methanol solution (10 mM) was added to 1 mL NWs suspension. After mixing 30 minutes, the mixture was dropped on silicon wafer and air-dried. It was rinsed 2-3 times with ethanol before Raman spectrum collection. SERS spectra

were obtained using a laser confocal Raman spectrometer (Invia plus, Renishaw) with 785 laser power.

Catalytic Hydrogenation Experiment.

The hydrogenation of phenol was carried out in a conical flask (50 mL) equipped with a magnified stirrer under flowing hydrogen. Typically, phenol solution was purged with flowing H₂ before adding catalysts into the flask. For all reactions, the reaction mixture contained phenol (0.03 mmol), water (30 mL), and freshly synthesized NWs catalysts (1 mol% of Rh+Pd relative to phenol), and the reaction was conducted at 25°C under a headspace flow of hydrogen and stirred at 300 rpm. Four parallel experiments were set up for each catalytic experiment, and samples taken at certain time were analyzed in an Agilent HPLC (1200) instrument with a C18 column for phenol detection and in an Agilent GC-MS (7890 A, 5975C) instrument with a HP-5MS column for products detection after CH₂Cl₂ extraction.

In the enlarged hydrogenation reaction of phenol and cresol, 30 mL reaction mixture contained 0.6 mol phenol/cresol and 1 mol% Rh + Pd relative to substrates. Except that, other conditions are the same as the above reaction conditions. In the stability test of catalysts, the spent catalyst was recovered by filtration, washed with methanol, and reused for the next run.

Raman Experiment of Phenol Adsorption on NWs

To enhance the Raman spectrum of adsorbed phenol on NWs, the NWs were loaded on Au@SiO₂-NH₂. The Au@SiO₂-NH₂ was synthesized according to Xie group.² Briefly, the mixture of Au colloid (1 mL, 0.25 mM), sodium citrate solution (10 μL, 1%) and MPTMS ethanol solution (10 μL, 10%) was stirred in a temperature-controlled shaker for 1h (50 °C, 750 rpm). After washed 2 times with water, sodium silicate solution (7 μL, 0.054%) was added into the suspension (1 mL). The mixture was incubated at 90°C (750 rpm) for 1 h and then washed 2 times with water. Finally, ammonia solution (50 μL 25%) and MPTMS (5.0 μL 10 %) were

added to the suspension (1 mL) and the mixture incubated at room temperature for 30 minutes and washed twice with water.

The Au@SiO₂-NH₂-NWs was synthesized by mixing NWs (200 μL) and Au@SiO₂-NH₂ suspension (1 mL) at room temperature for 30 min. Then, the mixture was washed twice and redispersed with water (Figure S19).

In the Raman experiment of adsorbed phenol on NWs, the suspension above was dropped on silicon wafer and air-dried. Then the silicon wafer was placed in phenol solution (1 mM) for collection of Raman spectrum.

Computational Method

The configurations of phenol adsorption on different surface were according to previous study.² Geometry optimization and energy calculation were performed using Vienna Ab Initio Simulation Package (VASP).^{3, 4} A 4 × 4 supercell and four layered slabs were built for all adsorption configurations. The adsorption energy was calculated according to the following equation:

$$E_{\text{ads}} = E_{(\text{phenol/surface})} - E_{(\text{phenol})} - E_{(\text{surface})}$$

Where $E_{(\text{phenol/surface})}$ is total energy of adsorbed phenol on slab, $E_{(\text{phenol})}$ is the energy of phenol, $E_{(\text{surface})}$ is the energy of slab.

Additional Discussions

Based on the cylindrical model and our previous result,⁵ if the added metal (Pd or Rh) precursor would be totally reduced and deposited onto Au NWs core, 0.3 molar equivalent of Rh/Pd (relative to Au) is sufficient to form a ML on Au surface, and this value is adopted in the whole studied. Diameter analysis indicates an accretion of approximately 0.5 nm for Au@Rh (4.06 nm) compared to Au NWs (3.49 nm), which matches well with the formation of an atomic Rh monolayer (ML) on the Au surface (Fig. S1). Centrifugation separation followed by ICP-MS analysis further revealed that more than 98% of the added RhCl_3 was reduced and deposited onto the Au NWs (Table S1). We further take advantage of the high sensitivity of the SERS spectra of chemisorbed 2,6-DMPI. Ideally, if a ML is formed on the surface of Au NW, the Au-related Raman band at 2170 cm^{-1} would be replaced by that of Pd- or Rh-related Raman band. This is true for Au@Pd, with the deposition of Pd layer on Au NWs, the Raman band assigned to the gold site bounded 2,6-DMPI weakens gradually and eventually disappears on Au@Pd_{1ML}, indicating the formation of Pd ML on the Au NWs (Figure S4). While for the case of Rh, the Raman band associated with vibration of $\text{N}\equiv\text{C}$ (ν_{NC}) that adsorbed onto Rh site is very close to that of Au, makes the directly differentiates Rh from Au atom a challenging work. However, the new Raman band at 420 cm^{-1} which is attributable to $\nu_{(\text{Rh}-\text{C})}$ confirms the formation of Au@Rh. Otherwise, the Raman band of 2,6-DMPI chemisorbed onto Rh could not be effectively enhanced (Fig. 3E). For RhPd overlayer, the co-existence of the Pd-related Raman band at 2000 and 2120 cm^{-1} and the Rh-related Raman band at 420 cm^{-1} infers the both Pd and Rh atoms co-deposited onto Au surface as bimetallic monolayer.

To further exclude the possibility that Rh and Pd atoms deposited onto different Au NWs and exists as Au@Pd and Au@Rh NWs mixture, we performed CO-stripping experiment (Fig. 1E

and S5). Compared with Rh/C, Au@Rh showed higher CO-stripping potential, subjects to the enhanced binding of CO to Rh sites. While for the RhPd mixture overlayer, the CO-stripping peak is between that of Au@Rh and Au@Pd, demonstrating the modulated binding strength of CO onto Rh and Pd sites.

Supporting Figures

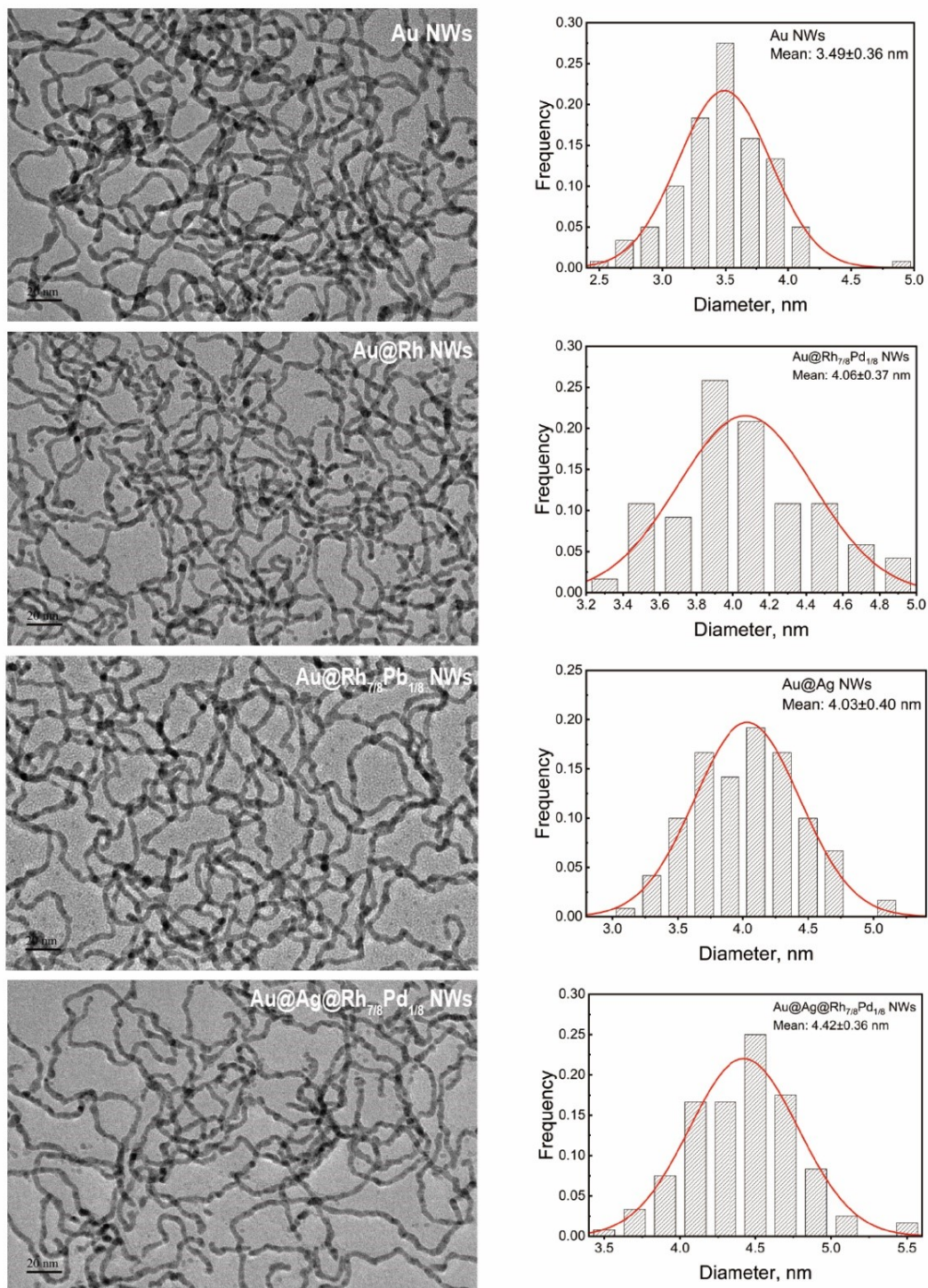


Figure S1. TEM images and diameter distribution of Au NWs, Au@Rh NWs, Au@Rh_{7/8}Pd_{1/8} NWs, Au@Ag@Rh_{7/8}Pd_{1/8} NWs.

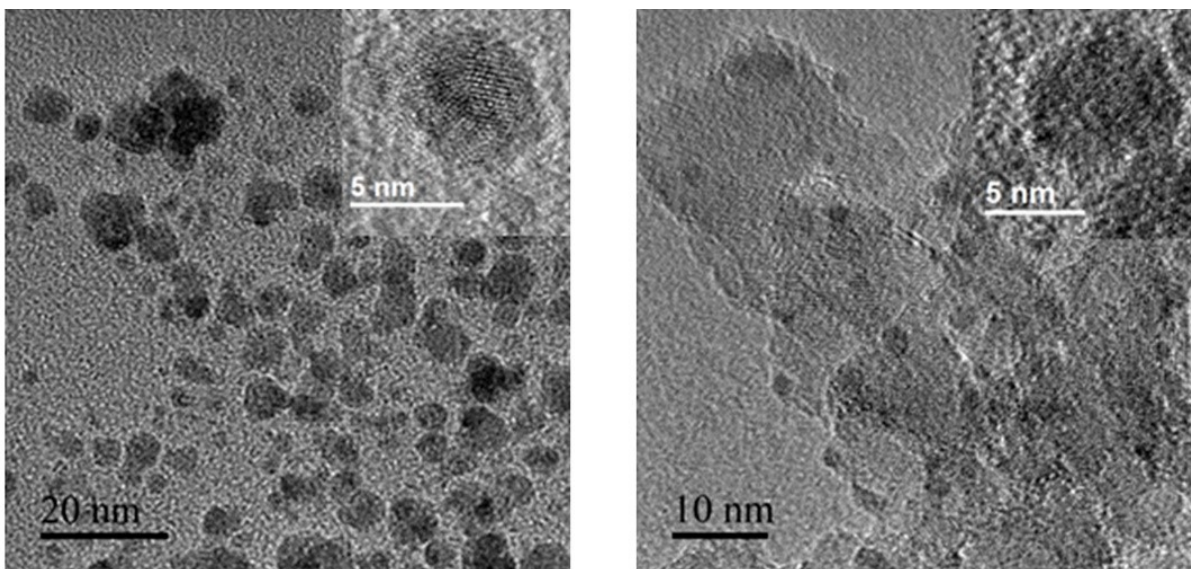


Figure S2. TEM images of Rh nanoparticles (left), commercial Rh/Al₂O₃ (right).

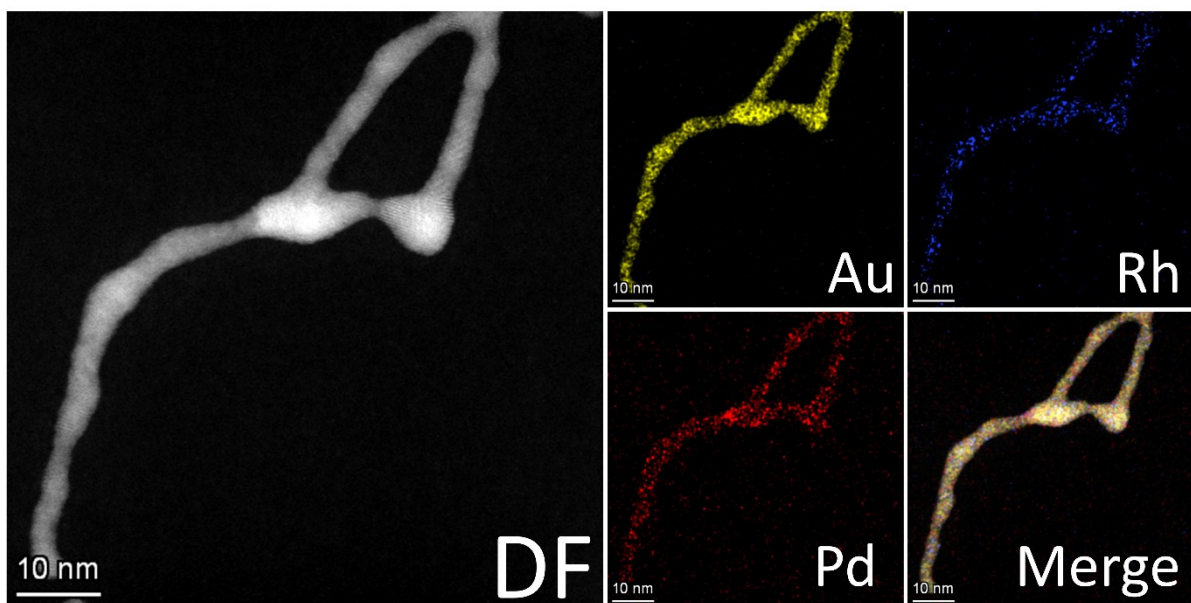


Figure S3. EDS mapping of A@Rh_{1/2}Pd_{1/2}.

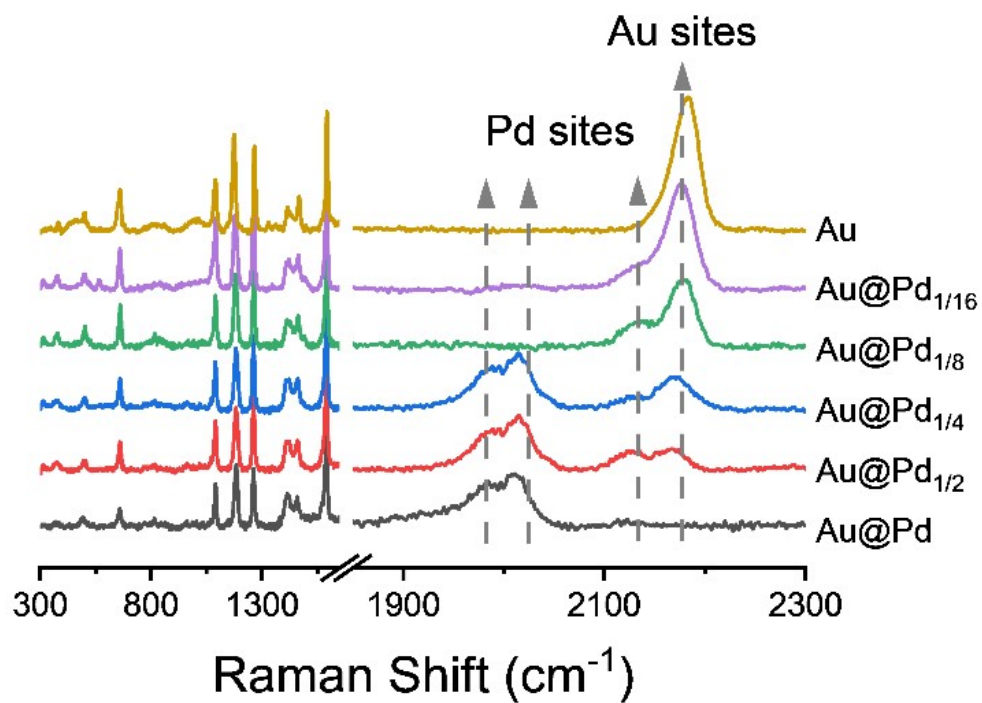


Figure S4. SERS spectra of chemisorbed 2,6-DMPI on Au@Pd NWs with different Pd coverage.

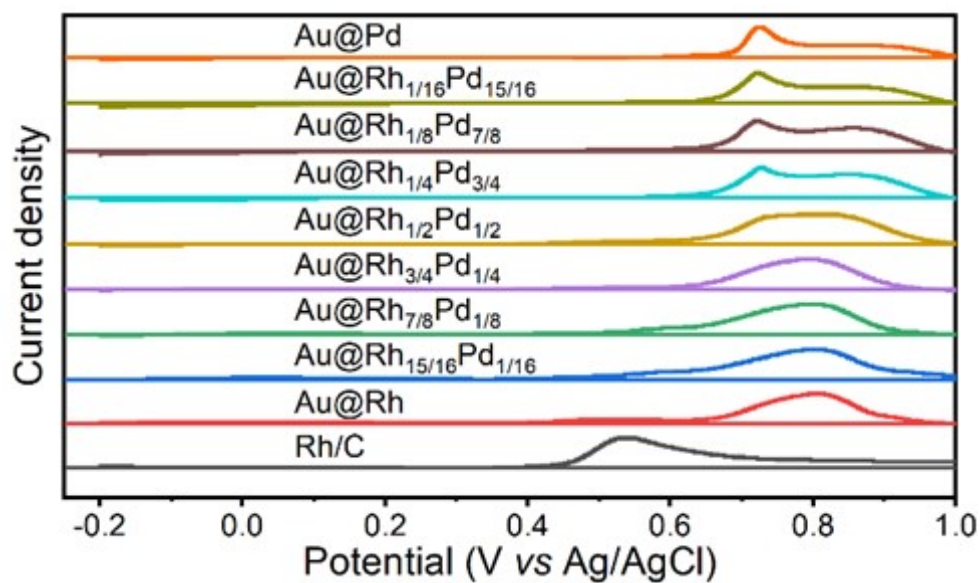


Figure S5. CO stripping voltammetry of different catalysts.

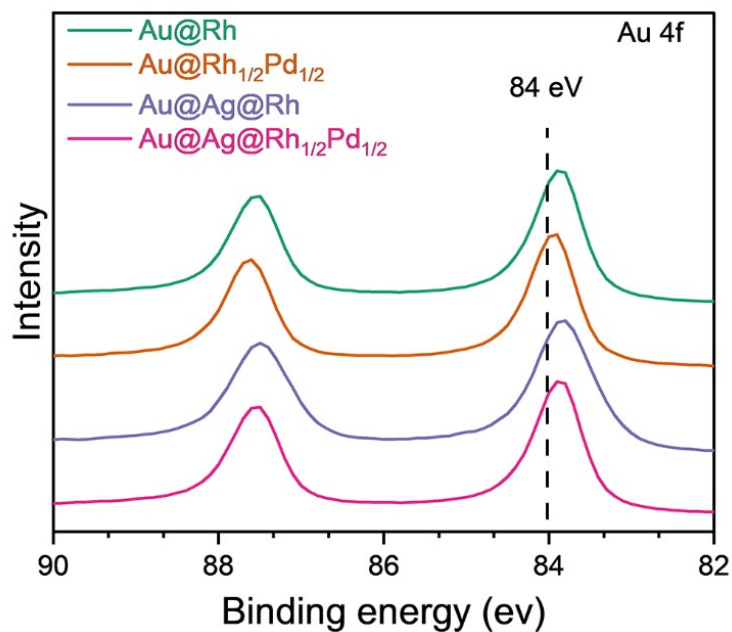


Figure S6. Au 4f core level XPS spectra.

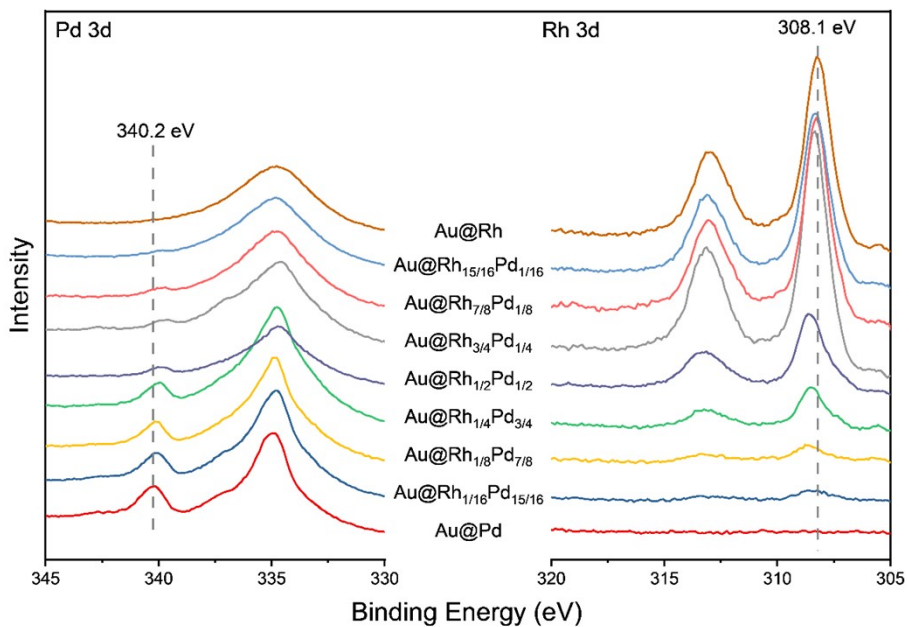


Figure S7. Pd 3d and Rh 3d core level XPS spectra of Au@RhPd NWs.

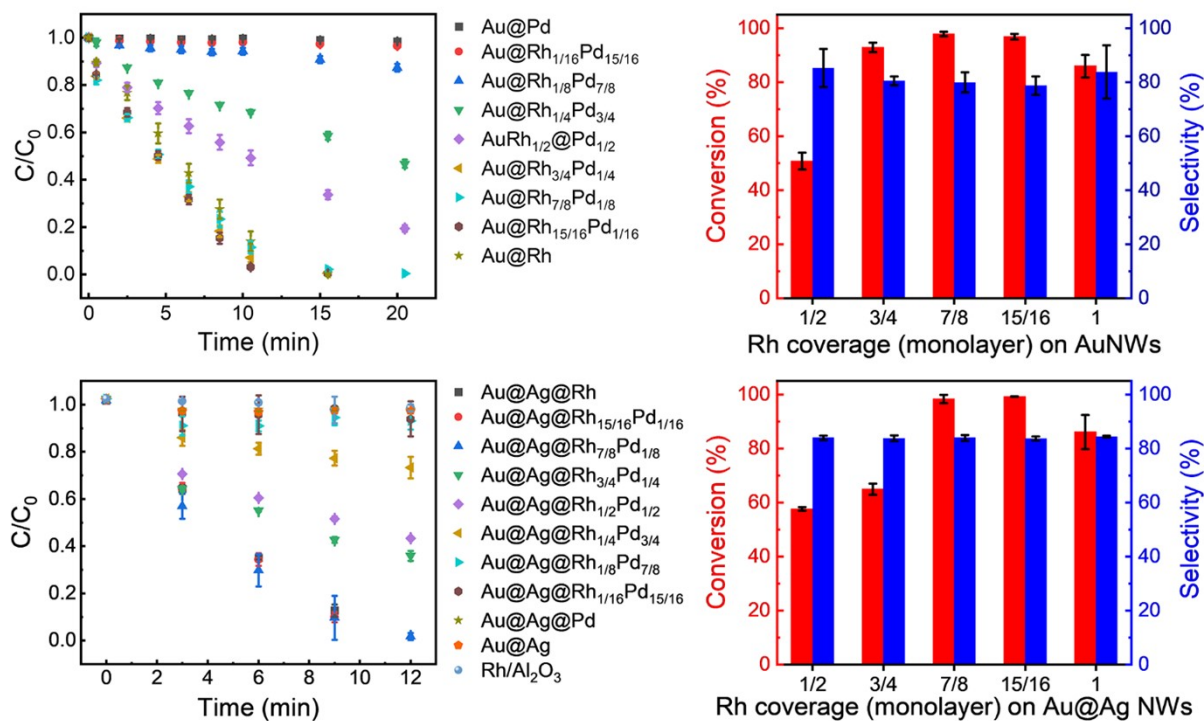


Figure S8. Catalytic performance of Au@RhPd NWs and Au@Ag@RhPd NWs, respectively.

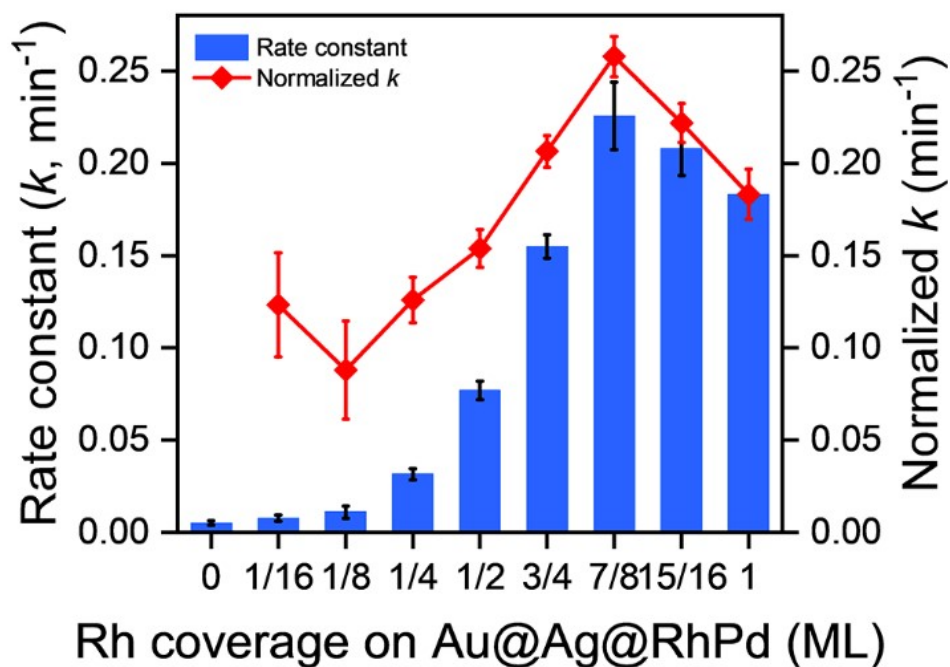


Figure S9. Calculated rate constant for Au@Ag@RhPd catalysts.

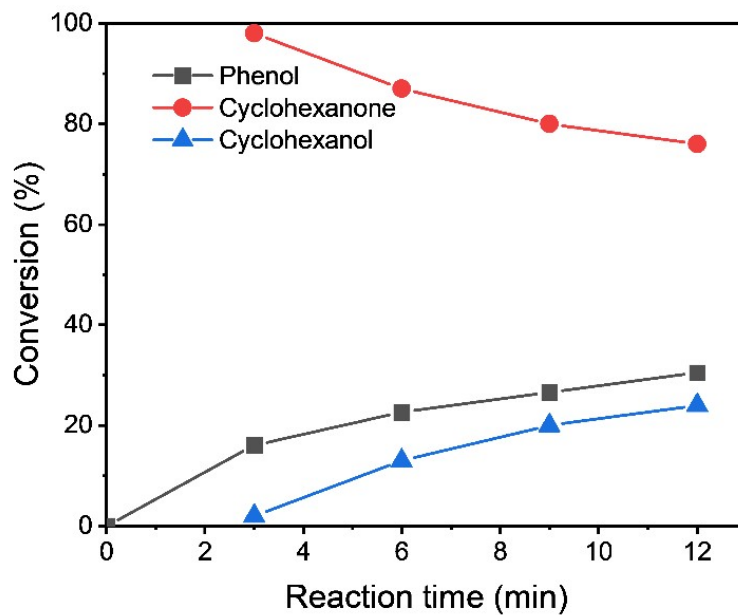


Figure S10. Time-dependent catalysis by Rh/Al₂O₃-H₂.

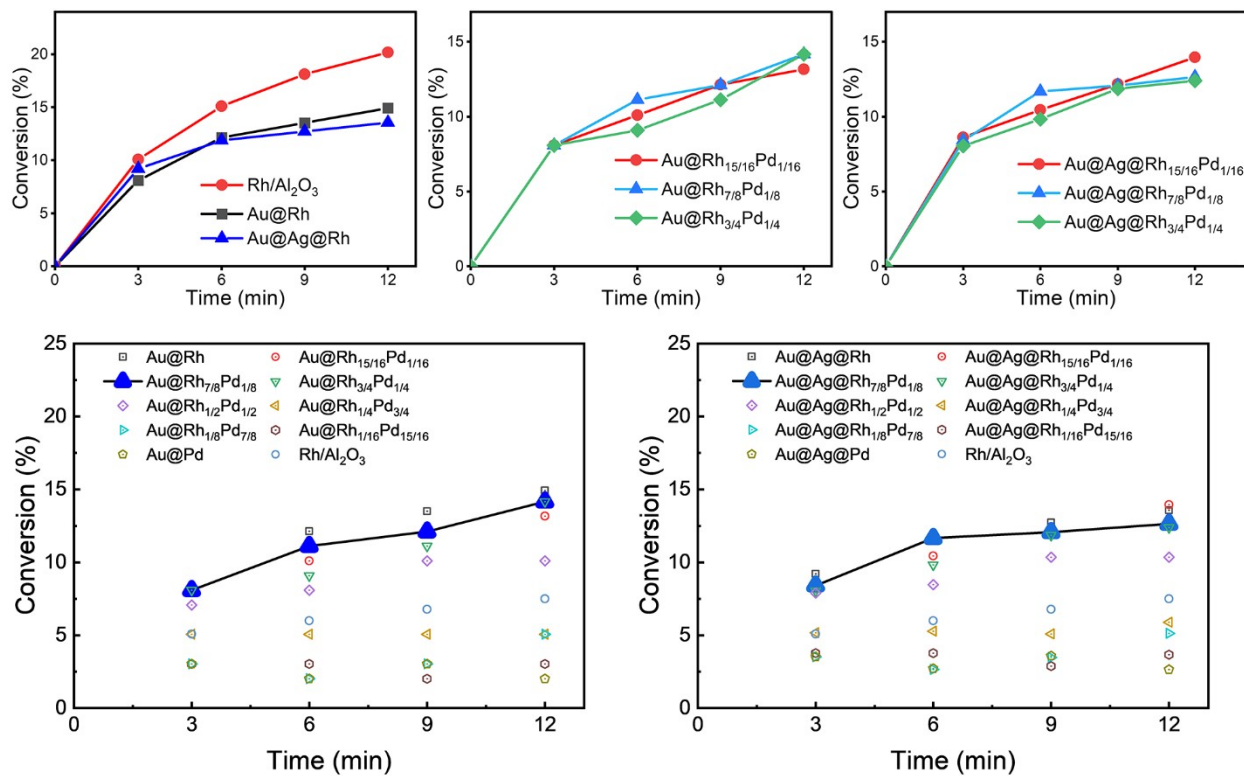


Figure S11. The hydrogenation of cyclohexanone catalyzed by Au@RhPd and Au@Ag@RhPd catalysts.

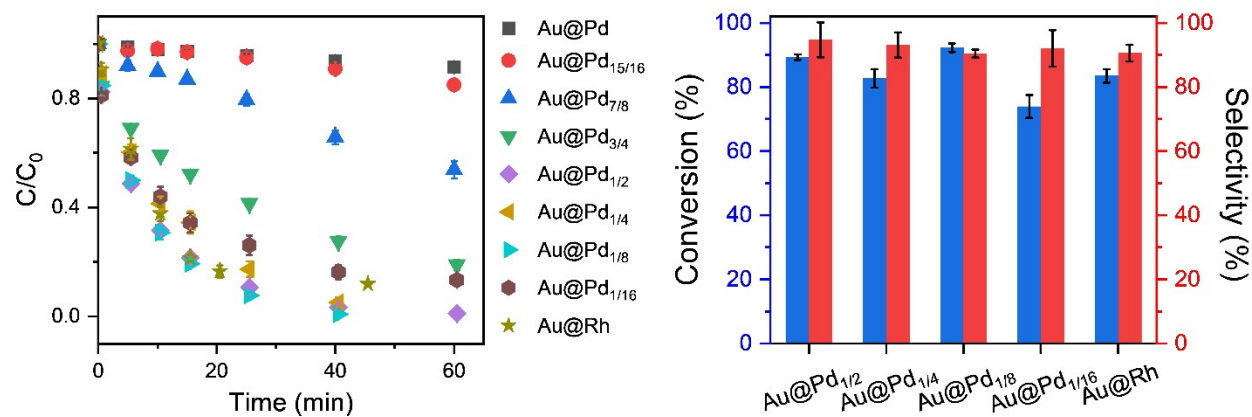


Figure S12. Catalytic performance of Au@RhPd catalysts with addition of NaOH.

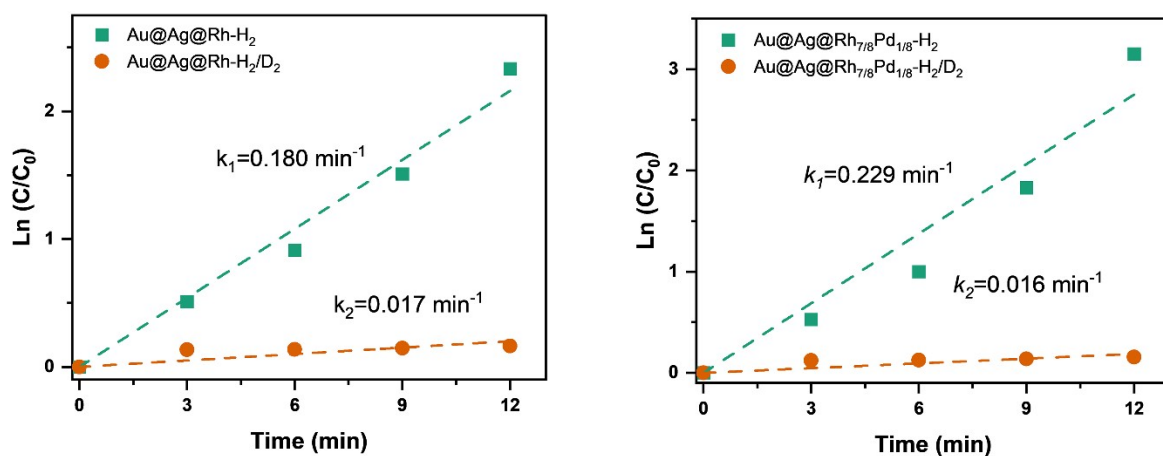


Figure S13. Primary isotope effect observed for Au@Ag@Rh and Au@Ag@Rh_{7/8}Pd_{1/8} in phenol hydrogenation.

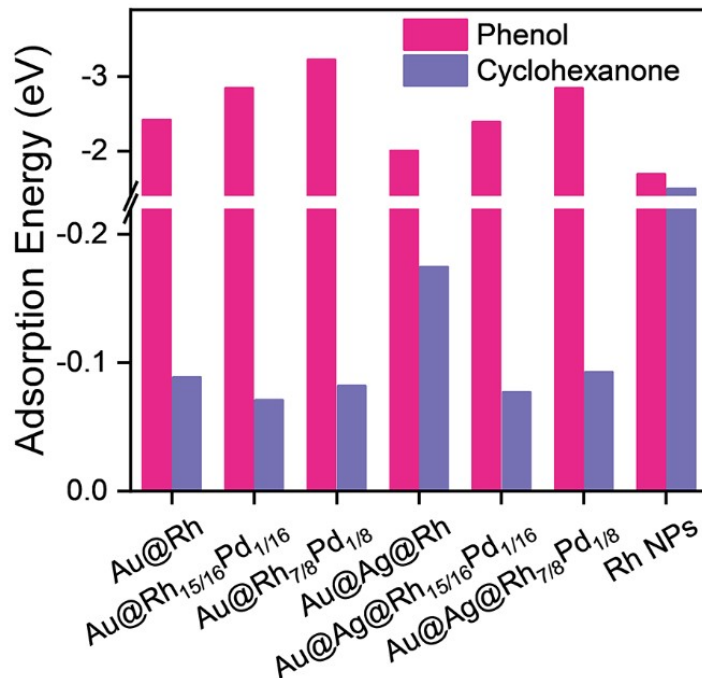


Figure S14. The calculated adsorption energy of phenol and cyclohexanone on different Rh-based catalysts.

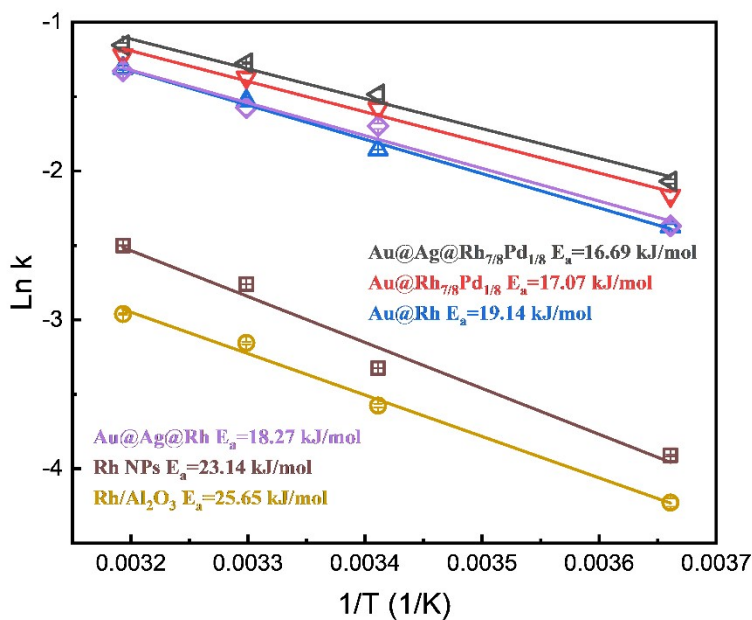


Figure S15. Arrhenius activation energy (E_a) of phenol and cyclohexanone on different Rh-based catalysts.

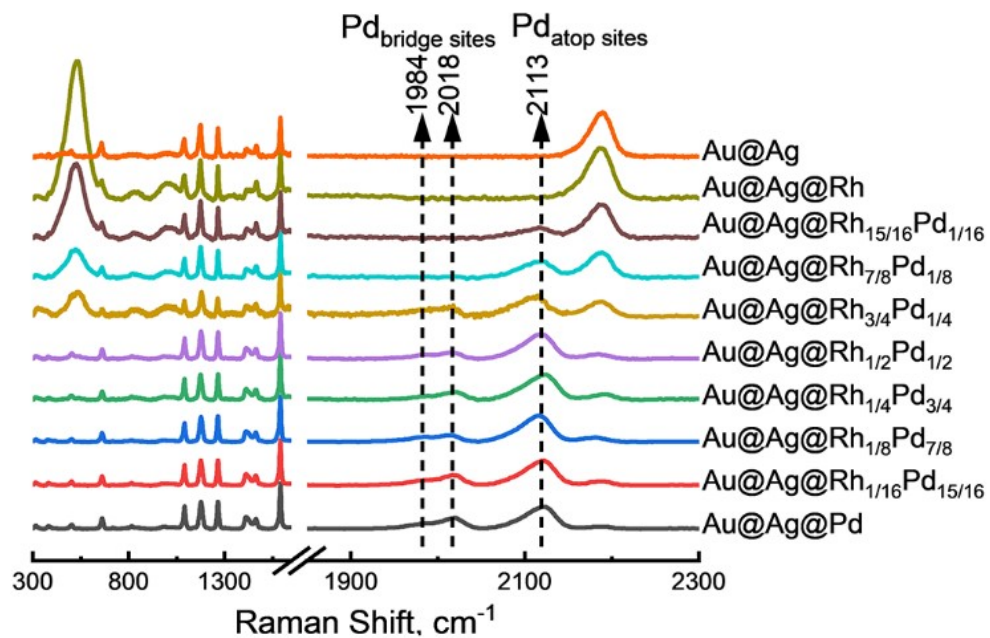


Figure S16. SERS spectra of chemisorbed 2,6-DMPI on Au@Ag@RhPd NWs.

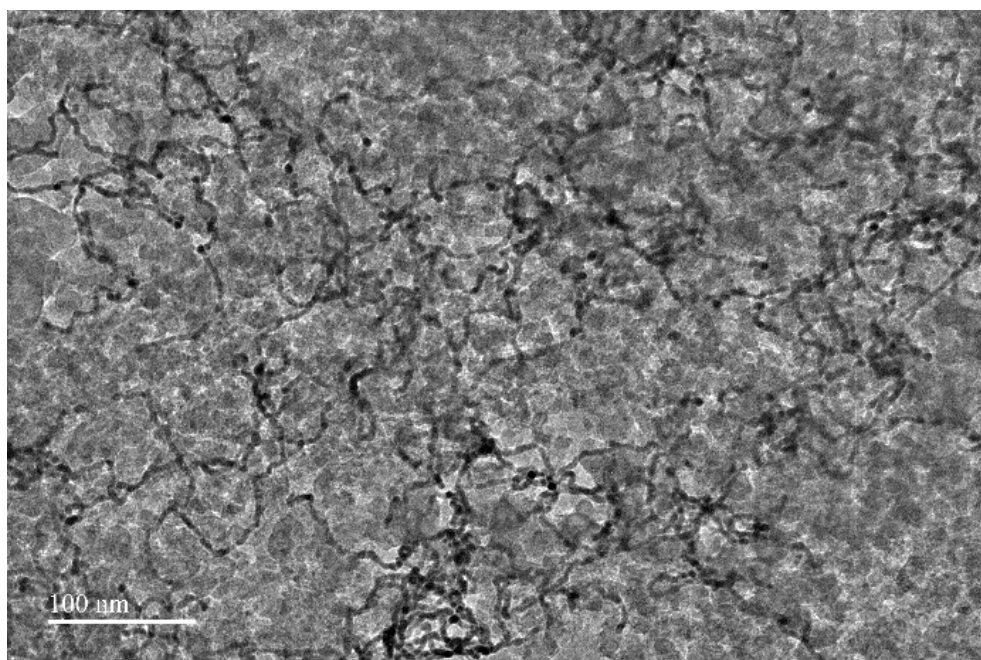


Figure S17. TEM image of NWs on SiO₂.

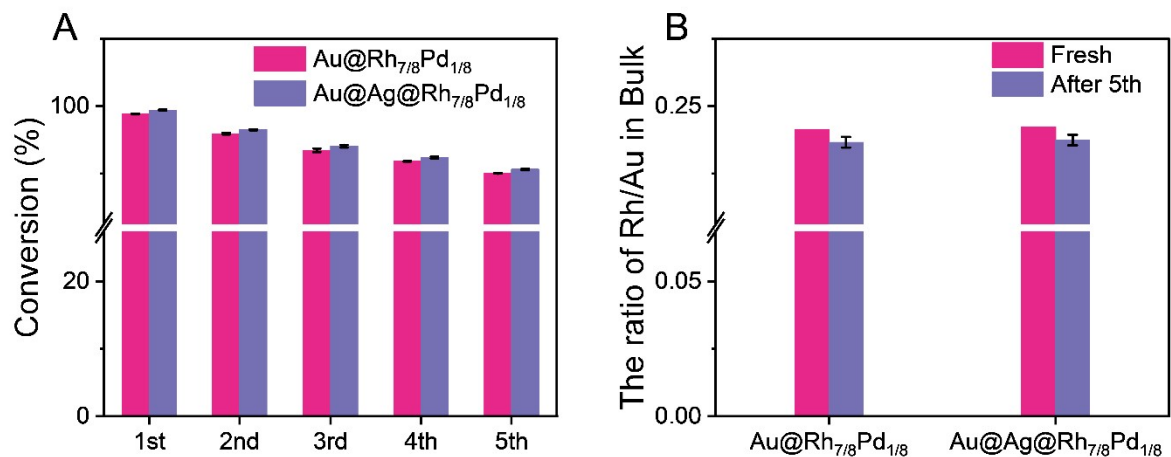


Figure S18. (A) The stability test of Au@Rh_{7/8}Pd_{1/8} and Au@AgRh_{7/8}Pd_{1/8}. (B) The ratio of Rh/Au in bulk catalysts before and after 5 uses.

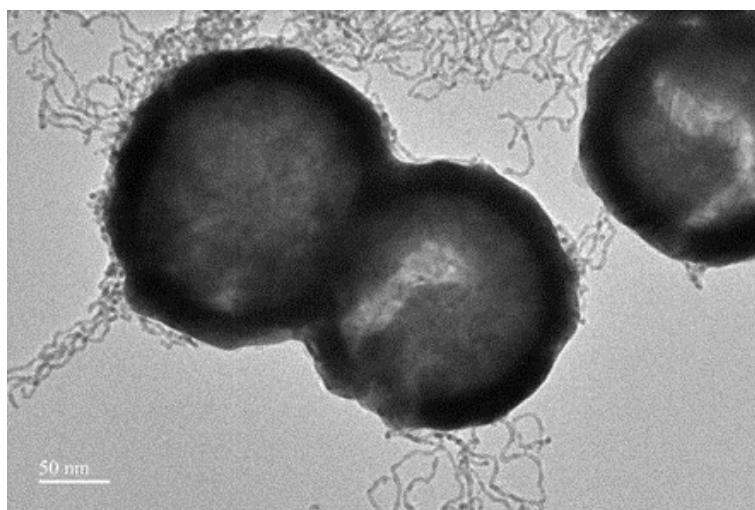
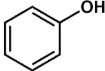
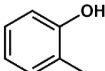
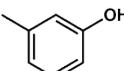
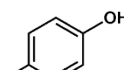
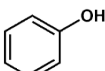
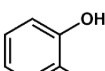
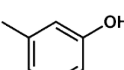
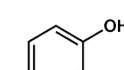
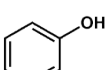


Figure S19. TEM image of Au@SiO₂-NH₂-NWs.

Table S1. ICP-OES analysis of Au@RhPd and Au@Ag@RhPd NWs.

	Theoretical Ratio of Rh/ (Rh + Pd)	Experimental Ratio of Rh/ (Rh + Pd)
Au(@Ag)@Rh	1	0.9944 (0.9961)
Au(@Ag)@Rh _{15/16} Pd _{1/16}	0.9375	0.9331 (0.9346)
Au(@Ag)@Rh _{7/8} Pd _{1/8}	0.875	0.8701 (0.8710)
Au(@Ag)@Rh _{3/4} Pd _{1/4}	0.75	0.7455 (0.7465)
Au(@Ag)@Rh _{1/2} Pd _{1/2}	0.5	0.5009 (0.5006)
Au(@Ag)@Rh _{1/4} Pd _{3/4}	0.25	0.2516 (0.2499)
Au(@Ag)@Rh _{1/8} Pd _{7/8}	0.125	0.1295 (0.1301)
Au(@Ag)@Rh _{1/16} Pd _{15/16}	0.0625	0.0631 (0.0618)
Au(@Ag)@Pd	0	0.0009 (0.0012)

Table S2. Hydrogenation of Phenol and Cresol catalyzed by Au@Rh_{7/8}Pd_{1/8} NWs and Au@Ag@Rh_{7/8}Pd_{1/8} NWs.^a

Entry	Substrate	Time (h)	Conv. (%)	Sel. ^b (%)	TOF (h ⁻¹)
1 ^c		2	98.9	82.5	565.2
2 ^c		5	90.2	86.9	206.2
3 ^c		4	92.7	88.3	264.9
4 ^c		2.5	96.9	84.3	443.1
5 ^d		2	99.3	83.9	567.5
6 ^d		5	94.7	84.1	216.6
7 ^d		4	93.1	84.3	266.0
8 ^d		2.5	97.4	83.9	445.3
9 ^e		2	95.3	81.1	552.4

[a] Reaction conditions were as follows: phenol, 0.6 mmol; Rh and Pd, 1 mol% relative to substrate; temperature, 25 °C; solvent, 30 mL of H₂O. [b] Chemoselectivity to substituted cyclohexanones. Entry 1-4 were catalyzed by Au@Rh_{7/8}Pd_{1/8} NWs and Entry 5-8 were catalyzed by Au@Ag@Rh_{7/8}Pd_{1/8} NWs. Entry 9 was catalyzed repeatedly by Au@Rh_{7/8}Pd_{1/8} NWs after entry 1.

Table S3. ICP-MS analysis of Au@Rh_{7/8}Pd_{1/8} and Au@Ag@Rh_{7/8}Pd_{1/8} before and after repeated uses.

	Before use		After 5 uses		Change in Au	Change in Rh/Au
	Au (mM)	Rh/Au	Au (mM)	Rh/Au		
Au@Rh _{7/8} Pd _{1/8}	0.158	0.241	0.150	0.236	- 4.82%	- 1.17%
Au@Ag@Rh _{7/8} Pd _{1/8}	1.130	0.242	1.124	0.237	- 4.85%	- 0.76%

Reference

- (1) Liu, R.; Zhang, L. Q.; Yu, C.; Sun, M. T.; Liu, J. F.; Jiang, G. B. Atomic-Level-Designed Catalytically Active Palladium Atoms on Ultrathin Gold Nanowires. *Adv. Mater.* **2017**, *29* (7), 1604571.
- (2) Hu, C.; Hu, Y.; Fan, C.; Yang, L.; Zhang, Y.; Li, H.; Xie, W. Surface-Enhanced Raman Spectroscopic Evidence of Key Intermediate Species and Role of NiFe Dual-Catalytic Center in Water Oxidation. *Angew. Chem. Int. Ed. Engl.* **2021**, *60* (36), 19774-19778.
- (3) Kresse, G.; Hafner, J. Ab initio molecular dynamics for liquid metals. *Phys Rev B Condens Matter* **1993**, *47* (1), 558-561.
- (4) Kresse, G.; Furthmuller, J. Efficiency of ab-initio total energy calculations for metals and semiconductors using a plane-wave basis set. *Computational Materials Science* **1996**, *6* (1), 15-50.
- (5) Liu, R.; Chen, H. M.; Fang, L. P.; Xu, C.; He, Z.; Lai, Y.; Zhao, H.; Bekana, D.; Liu, J. F. Au@Pd Bimetallic Nanocatalyst for Carbon-Halogen Bond Cleavage: An Old Story with New Insight into How the Activity of Pd is Influenced by Au. *Environ Sci Technol* **2018**, *52* (7), 4244-4255.